

CHARACTERISTIC VELOCITY AND MASS TRANSFER IN ROTATING IMPELLER COLUMN

Dong Kwon Kum, Yeong Min Jeon and Won Kook Lee*

Department of Chemical Engineering
 Korea Advanced Institute of Science and Technology
 P.O. Box 131 Dongdaemun, Seoul 130, Korea
(Received 30 April 1985 • accepted 24 May 1985)

Abstract— The effects of system variables on flow characteristics and mass transfer rate were studied in a rotating impeller column using a ternary system of water (continuous phase)-acetone (solute)-cyclohexane (dispersed phase). The characteristic velocity, Peclat numbers in both phases and mass transfer coefficient between phases were correlated as;

$$\begin{aligned}\bar{U}_o &= 6.3 (10^2) (Nd_I)^{-2.1} Z_c^{0.83} \\ \frac{\bar{U}_c L}{D_c} &= 1.26 N^{-1.11} d_I^{-2.17} Z_c^{-0.59} \bar{F}_c^{1.9} \\ \frac{\bar{U}_d L}{D_d} &= 20.5 N^{-0.78} d_I^{-1.36} Z_c^{-0.25} \bar{F}_c^{0.09} \\ \frac{k_{local} L}{\bar{U}_d} &= 13.2 N^{1.33} d_I^{0.74} Z_c^{-0.93} \bar{F}_c^{-0.78}\end{aligned}$$

INTRODUCTION

The extraction columns used in industry or studied in laboratories are pulsed-packed column, pulsed-plate column, reciprocating plate column, rotary disc column (RDC), and Oldsue-Rhuston column (or Mixco column). RDC and Mixco column have been more commonly used because of such advantages that: (1) mass transfer efficiency is larger than other equipments, (2) maintenance and operating cost are low, (3) the structure is simpler, and especially, (4) loss of efficiency due to scale-up small.

The study on axial mixing of the dispersed phase and continuous phase has been done by Misek [6], Strand et al. [13], Zhang et al. [16], and Westerterp and Landsman [15] for RDC and by Biband and Treybal [1] for Mixco column. In the study for RDC the effects of system variables on mass transfer coefficient were investigated by Vermijs and Krammers [14] and the mass transfer efficiency was expressed in terms of power number by Reman and Olney [12] and also Logsdail [5] reported correlation equations for designing the RDC using various materials. The degree of mixing between stages was also studied by Miyauchi et al.[8] for RDC

and Mixco column, and by Edgar [2] for Mixco column. Strand et al.[13] obtained an empirical equation for maximum drop size in RDC and Logsdail [5] and Mumford [9] reported equations for average drop size in the column.

The rotating impeller column without baffles has almost not been studied. The object of this study is to investigate the effects of system variables on hydrodynamics and mass transfer in a rotating impeller column.

MODELS

Flow Characteristics

The characteristic velocity has been used for the study of hydrodynamics in liquid-liquid extraction column, which is defined to be the mean velocity of droplets with respect of the continuous phase. It had been developed by Pratt [11] in packed column, but it has been used in almost all extraction columns after being applied to RDC by Logsdail [5]. The relation of the characteristic velocity to dispersed phase hold-up was proposed by Kung [3] as follow:

$$\frac{\bar{U}_d}{h} + \frac{\bar{U}_c}{1-h} = \bar{U}_o (1-h) \quad (1)$$

for $(d_s - d_I)/d_T > 1/24$. The characteristic velocity can be

*To whom all correspondence should be addressed.

obtained from plot of $h(1-h)$ versus $(\bar{U}_a + \frac{h}{1-h}\bar{U}_c)$.

Mass Transfer

The approaches to the problem of backmixing are usually described by mathematical models in two different ways. The first is the stagewise backmixing models [10] which is assumed that each stage is perfectly mixed, but it is not possible to distinguish the axial mixing in two phase. The second approach is the differential backmixing models (DBM) [7] which describes mass transfer in countercurrent continuous equipment with axial mixing. The axial mixing effect is expressed by means of the Peclet numbers. Although both models give approximately equal results under the highly dispersive conditions commonly encountered in agitated column extractors, the differential backmixing model is most commonly preferred. Thus DBM is expressed by the following (Fig. 1):

$$-U_a \frac{dX}{dl} = -U_c \frac{dY}{dl} = m k_{oca} a (x - x^*) \quad (2)$$

where

$$U_a X = U_a \cdot x - D_a \frac{dx}{dl} \quad (3)$$

and

$$U_c Y = U_c \cdot y + D_c \frac{dy}{dl} \quad (4)$$

The Eq. (2) is expressed in terms of dimensionless groups to give:

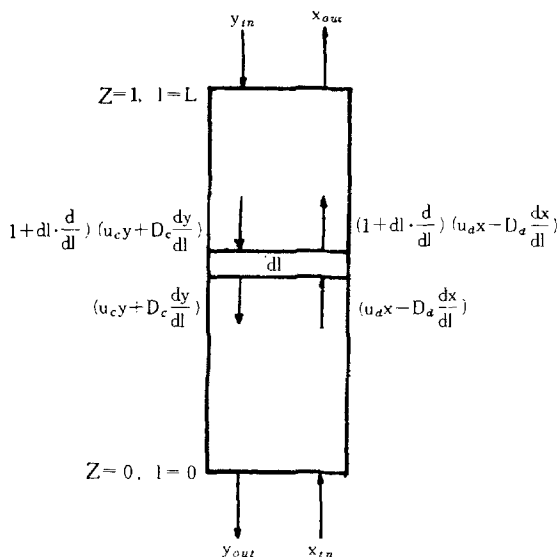


Fig. 1. Countercurrent differential backmixing model.

$$-\frac{dX}{dZ} = -\frac{1}{Q} \frac{dY}{dZ} = T(x - x^*) \quad (5)$$

where

$$X = x - \frac{1}{P} \left(\frac{dx}{dZ} \right), \quad Y = y + \frac{1}{R} \left(\frac{dy}{dZ} \right)$$

$$Z = \frac{1}{L}, \quad P = \frac{U_a L}{D_a}, \quad R = \frac{U_c L}{D_c},$$

$$T = \frac{m \cdot k_{oca} \cdot L}{U_a}, \quad Q = \frac{U_a}{U_c}$$

with boundary conditions;

$$x_{in} = X \quad \text{at } Z = 0 \quad (6)$$

$$\frac{1}{R} \left(\frac{dy}{dZ} \right) = 0 \quad \text{at } Z = 1$$

$$y_{in} = Y \quad \text{at } Z = 1 \quad (7)$$

$$\frac{1}{P} \left(\frac{dx}{dZ} \right) = 0 \quad \text{at } Z = 0$$

Eq. (5) is solved under the assumption of linear equilibrium relationship between two phases, i.e., $x^* = my$, to give [9]:

$$\frac{x_{in} - x}{x_{in} - my_{in}} = \frac{A + B(Z)}{A + FB} \quad (8)$$

and

$$\frac{my - my_{in}}{(x_{in} - my_{in}) F} = \frac{A(Z) + B}{A + FB} \quad (9)$$

where

$$A(Z) = \sum_1^3 g_1 g_3 \mu_1 e^{\mu_1} (\mu_2 e^{\mu_3 Z} - \mu_3 e^{\mu_2 Z}) \quad (10)$$

$$A = A(Z) \quad \text{at } Z = 0$$

$$B(Z) = \sum_1^3 g_1 \mu_1 e^{\mu_1} + \mu_3 (e^{\mu_3 Z} - \mu_3 e^{\mu_3 Z}) \quad (11)$$

$$B = B(Z) \quad \text{at } Z = 1$$

$$g_1 = (1 - \mu_1/P)(1 + \mu_1/R)$$

$$F = mQ = mU_a/U_c \quad (12)$$

The values of μ_1 , μ_2 and μ_3 can be obtained from the following equation:

$$\mu^3 - \mu^2 (R - P) - \mu (RP + TP + FRT) + TRP(F - 1) = 0 \quad (13)$$

The optimum values of P , R , T can be evaluated by comparing both concentration profiles with column height obtained from experiments and from Eq. (8) to Eq. (13). Details are found elsewhere [4].

EXPERIMENTAL APPARATUS AND PROCEDURE

Detail structure of the column used is shown in Figure 2. The column was made of two acryl cylinders with 13.2 cm ID and 60 cm length. Each compartment (or stage) was divided by stator rings with 10cm opening,

and the distance between them was changed from 7.0 cm to 12.0 cm. The impellers were four blades turbine type and the ratio of length to height of each paddle was unity. Drop generator was made about 100 capillaries with 0.119 cm ID and 0.150 cm OD.

The continuous phase (water) was fed from top and the dispersed phase (cycle hexane containing acetone as a solute) from bottom. The two phases flowed out opposite sides after contacting by the impeller rotation. After several tens of minutes elapsed (i.e., after steady state was achieved) the samples were extracted two steps. First, the continuous phase was very sampled slowly through the column at four points with direct observation so that the dispersed phase may not be en-

trained, and the second, the mixtures was quickly sampled at same positions that it contains the same quantity of the dispersed phase as in the column. The former four samples were to obtain concentration profile with column height and the latter four were sampled for the dispersed phase hold-up profile. The former four samples were analysed by Varian model 920 gas chromatograph with thermal conductivity detector and 4ft column of carbowax 20M. Each sample in the latter was collected directly into bottles which could measure density of liquids in them, so that the density difference between the liquid and the continuous phase gives the dispersed phase hold-up. The experimental ranges were as follows:

Impeller diameter	: 5.5-8.5 cm
Impeller speed	: 180-360 rpm
Compartment height	: 7.0 - 12.0 cm
CP flow rate	: 0.8 - 2.0 l/min
DP flow rate	: fixed to 0.1 l/min

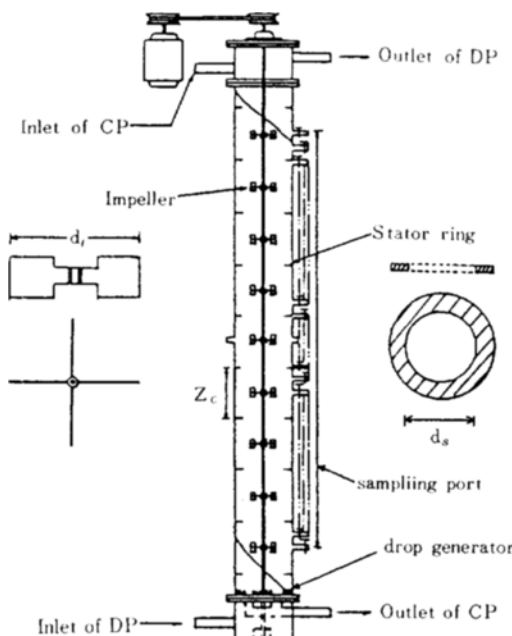


Fig. 2. Details of Rotating impeller column.

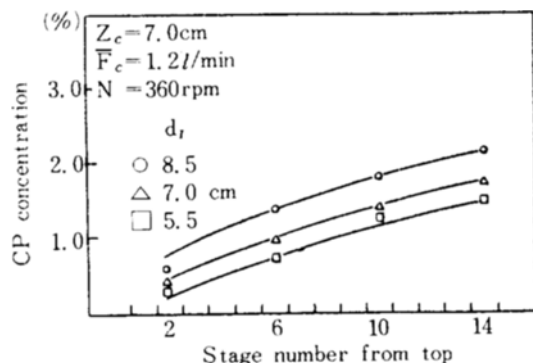


Fig. 3. Solute concentration profile in continuous phase.

RESULTS AND DISCUSSIONS

Fig. 3, 4, 5 and 6 show concentration profile with col-

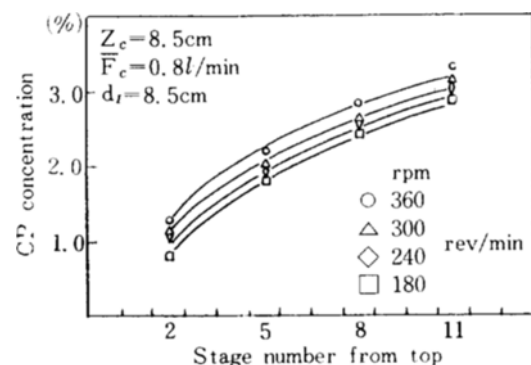


Fig. 4. Solute concentration profile in continuous phase.

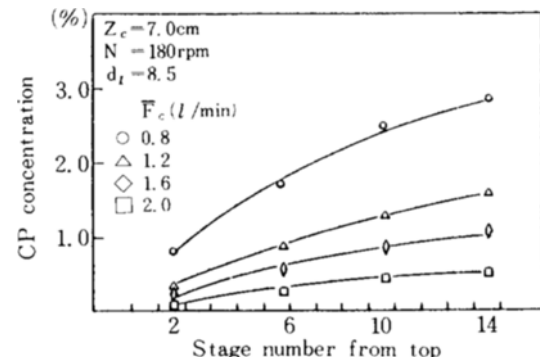


Fig. 5. Solute concentration profile in continuous phase.

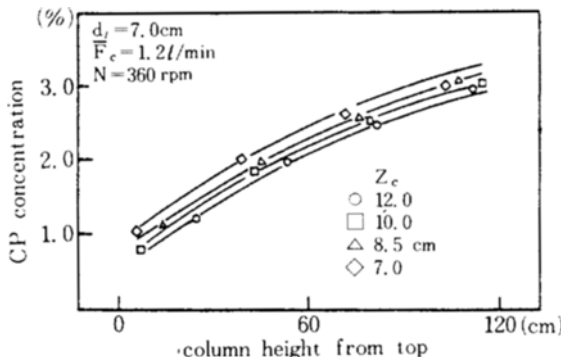


Fig. 6. Solute concentration profile in continuous phase.

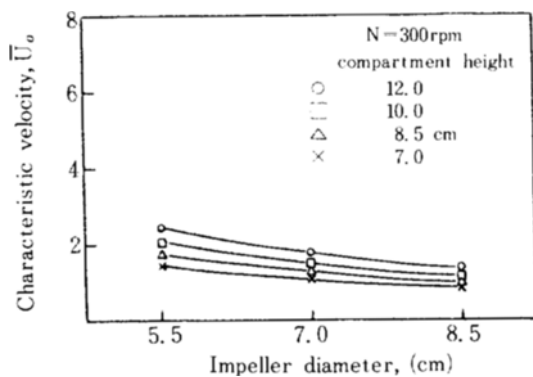


Fig. 7. Effect of impeller diameter on \bar{U}_o .

umn height at several experimental points and Fig. 7 and 8 show the effects of system variables on characteristic velocity. From these figures the mass transfer rate is found to be increased with increasing the impeller speed and the impeller diameter, and the characteristic velocity is shown to be decreased with increasing the impeller speed and the impeller size, and with decreasing the compartment height.

Eq. (1) suggests that the slopes of the plots h ($1-h$) vs $(\bar{U}_d + \frac{h}{1-h} \bar{U}_c)$ give the values of characteristic velocity, \bar{U}_o , of the drops through the column. The velocity is the function of the rotor speed, impeller size and compartment height. Thus, the characteristic velocity obtained from Eq. (1) was found to have the following relation with system variables:

$$\bar{U}_o = 6.3 \cdot 10^2 (Nd_i)^{-2.1} Z_c^{0.83} \quad (14)$$

which is correlated in Figure 9. The characteristic velocity is compared with that obtained from RDC in Figure 10. In RDC, the characteristic velocity \bar{U}_o is nearly independent of rotor speed in low rotor speed region. It can be explained that the moving dispersed drops is merely deflected by the rotating disks without causing any appreciable breakup of the drops, as the difference

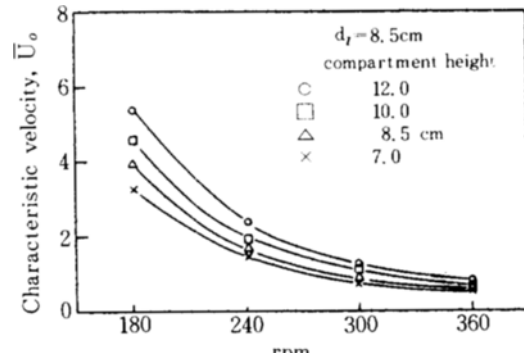


Fig. 8. Effect of RPM on \bar{U}_o .

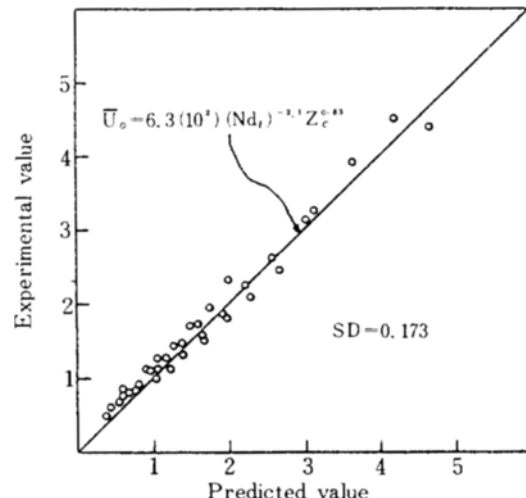


Fig. 9. Correlation of characteristic velocity.

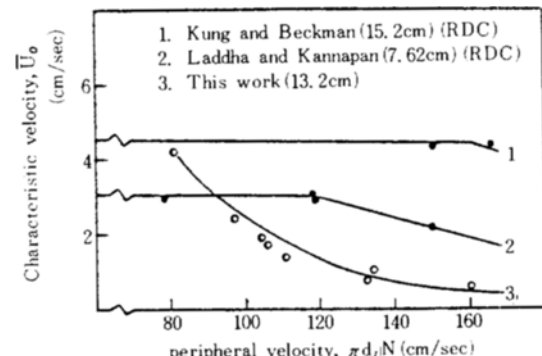


Fig. 10. Effect of peripheral velocity on \bar{U}_o .

in dynamic pressure created may not be sufficient to overcome the interfacial tension force. But, the impeller type used in this study has higher mixing effect than disk type, as shown Fig. 12. As the rotor speed increases, the energy spent at impeller, also increases markedly, and the interfacial tension is overcome, thereby

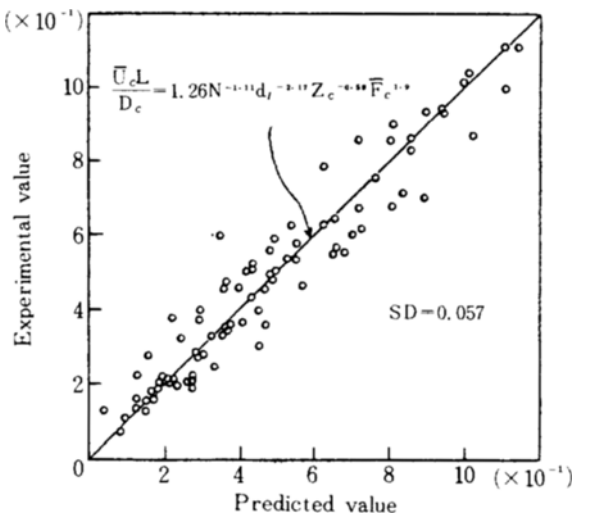


Fig. 11. Correlation of Peclet number of continuous phase.

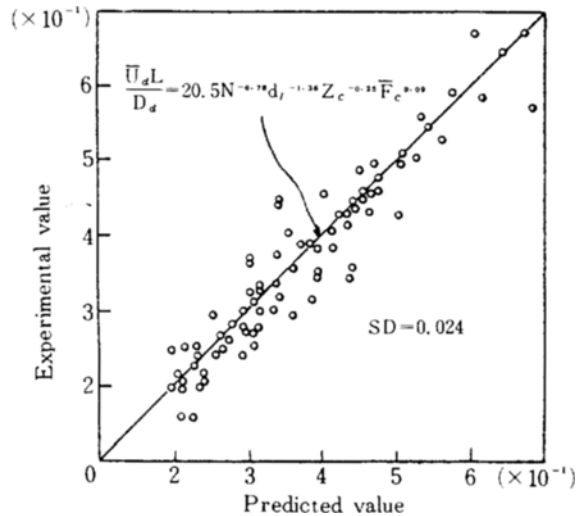


Fig. 13. Correlation of Peclet number of dispersed phase.

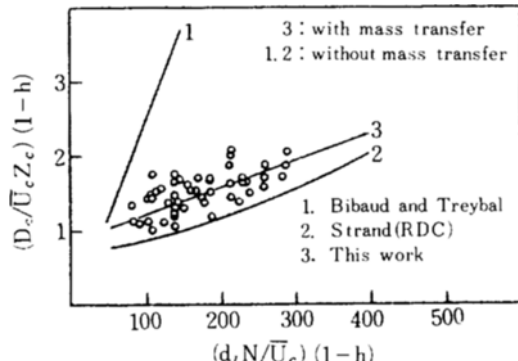


Fig. 12. Axial dispersion coefficient of continuous phase.

resulting in drop breakup in addition to enhancing the tortuous path of drops.

Thus the characteristic velocity shows a marked decrease with increasing rotor speed.

The optimum values of system parameters (P , R and T) appeared in Eq (8)-(13) obtained by using a nonlinear regression method [4] with the concentration profile obtained from experiments, and they were correlated with system variables. The continuous phase Peclet number was correlated in Figure 11 to give the following empirical equation:

$$P_{e, c} = \frac{\bar{U}_c L}{D_c} = 1.26 N^{-1.11} d_i^{-2.17} Z_c^{-0.59} \bar{F}_c^{1.9} \quad (15)$$

From eq. (15) back mixing is found to be increased with increasing the impeller size, speed and compartment height, and decreased with increasing the continuous phase flow rate. The same tendency was found in RDC

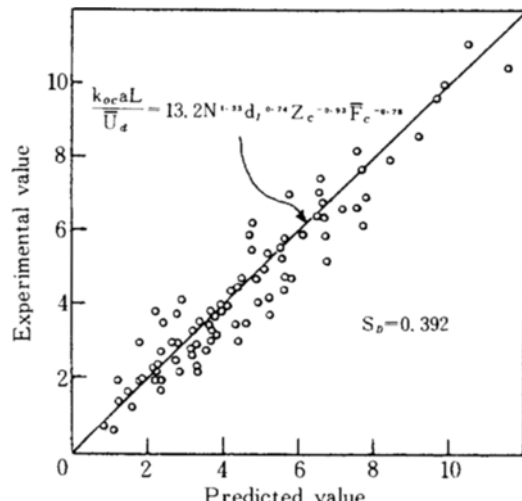


Fig. 14. Correlation of mass transfer coefficient based on continuous phase.

by Westerterp and Landsman [15]. The axial mixing coefficient in the continuous phase is compared with that obtained from Mixco column with six blades by Bibaud [1] and from RDC by Strand et al. [13] in Fig. 12. It can be found from this comparison that rotating impeller column has lower mixing effect than Mixco column but higher than RDC.

The dispersed phase Peclet number was correlated with system parameters as in Fig. 13 and the following relationship was found:

$$P_{e, d} = \frac{\bar{U}_d L}{D_d} = 20.5 N^{-0.78} d_i^{-1.36} Z_c^{-0.25} \bar{F}_c^{0.69} \quad (16)$$

The back mixing coefficient of the dispersed phase is found to show similar dependency on the impeller size, speed and compartment height as it in the continuous phase, but almost not affected by the continuous phase flow rate. The low inertia force of the small drops that are present at high rotor speeds and impeller size, may be enhanced to axial spreading. With increasing compartment heights (i.e. increasing stage volumes), the probability which can be occurred circulation to axial directions is increased. Thus the backmixing increases.

The mass transfer coefficient had the following relation with system variables:

$$\frac{k_{oc}aL}{\bar{U}_a} = 13.2 N^{1.33} d_I^{0.74} Z_c^{-0.93} \bar{F}_c^{-0.78} \quad (17)$$

which is correlated in Fig. 14 Mass transfer rate is shown to be increased with the impeller size and speed, and decreased with the compartment height and the continuous phase flow rate. With increasing impeller size and rotor speed the dispersed phase break into more smaller droplets so that mass transfer rate may be enhanced since the interfacial area is increased.

CONCLUSIONS

The dispersed phase hold-up and concentration profile of the continuous phase with height were measured in a rotating impeller column. The characteristic velocity was obtained from the data of the dispersed phase hold-up, and correlated with system variables. The Peclet number in the dispersed and the continuous phases, and mass transfer coefficient were obtained using the differential back mixing model. They were correlated with system variables.

The characteristic velocity and the continuous phase backmixing coefficient were compared with those obtained from other types of extraction column to find the difference of the column performance between the rotating impeller column and other columns. These correlations were expressed as:

$$\bar{U}_o = 6.3 (10^2) (Nd_I)^{-2.1} Z_c^{0.63}$$

$$\frac{\bar{U}_c L}{D_c} = 1.26 N^{-1.11} d_I^{-2.17} Z_c^{-0.59} \bar{F}_c^{1.9}$$

$$\frac{\bar{U}_d L}{D_d} = 20.5 N^{-0.78} d_I^{-1.36} Z_c^{-0.25} \bar{F}_c^{0.09}$$

$$\frac{k_{oc}aL}{\bar{U}_a} = 13.2 N^{1.33} d_I^{0.74} Z_c^{-0.93} \bar{F}_c^{-0.78}$$

NOMENCLATURE

a :effective interfacial area of contact between the phases, cm^2/cm^3
 d_I :impeller size, cm

d_s	:openings stator ring, cm
d_T	:column diameter, cm
d_{VS}	:sauter-mean volume to surface ratio of droplet, cm
D_d, D_c	:axial mixing coefficient of dispersed and continuous phases, respectively, cm^2/sec
F	:extraction factor, $m(\bar{F}_d/\bar{F}_c)$
\bar{F}	:superficial volume flow rates, cm^3/sec
g	:gravity acceleration, cm/sec^2
h	:hold up of dispersed phase
k_{oc}	:overall mass transfer coefficient based on continuous phases
L	:total length of extraction tower, cm
m	:distribution coefficient
N	:rotor speed, rev/sec
$P_{Pe,d}$:Peclet number of dispersed phases, $\bar{U}_d L/D_d$
Q	: U_d/U_c or F_d/F_c
$P_{Pe,c}$:Peclet number of continuous phases, $\bar{U}_c L/D_c$
S_D	:standard deviation
T	: $m \cdot k_{oc} \cdot L \cdot \bar{U}_d$
\bar{U}	:superficial velocity, cm/sec
\bar{U}_o	:characteristic velocity, cm/sec
x	:concentration of dispersed phases, g solute/100cc, water (solute free)
x^*	:x concentration in equilibrium with y
x_{in}	:x concentration of inlet
y	:concentration of continuous phases, g solute/100cc cyclohexane (solute free)
y_{in}	:y concentration at inlet
Z	:dimensionless length, 1/L
Z_c	:compartment height, cm
Greek Letters	
μ	:viscosity
ρ	:density
Subscription	
c	:continuous phase
d	:dispersed phase
m	:mixture
in	:inlet point

REFERENCES

1. Bibaud, R. B. and Treybal, R. B.: *AIChE J.*, **12**, 472 (1966).
2. Edgar, B. G.: *AIChE J.*, **19**, 712 (1973).
3. Kung, E. Y. and Beckman, R. B.: *AIChE J.*, **7**, 319 (1961).
4. Keum D. K. M.S. thesis KAIST (1984).
5. Logsdail, D. H., Thornton, J. D. and Pratt, H. R.C.: *Trans. Inst. Chem. Engrs.*, **36**, 301 (1957).
6. Misek, T.: *Coll. Czech. Chem. Comm.*, **28**, 426 (1963).
7. Miyauchi, T. and Vermulen, T.: *Ind. Eng. Chem.*

Fund., **2**, 304 (1963).

- 8. Miyauchi, T., Mitsutage, H. and Harase, I.: *AIChE J.*, **12**, 508 (1966).
- 9. Mumford, C. J., Al-homiri, A. A. A., Proc. Intern. Solvent Extrxn. Conf., Lyon (ISEC), **2**, 1591 (1974).
- 10. Mecklenburgh, J. C. and Hartland, S.: John Wiley & Sons, New York, 1975.
- 11. Pratt, H. R. C. and Gayler, R.: *Trans. Inst. Chem. Engrs*, **31**, 57 (1953).
- 12. Reman, G. H. and Olney, R. B.: *Chem. Eng. Prog.*, **51**, 141 (1955).
- 13. Strand, C. P., Olney, R. B. and Ackerman, G. H.: *AIChE J.*, **8**, 252 (1962).
- 14. Vermijs, H. J. A. and Krammers, H.: *Chem. Eng. Sci.*, **3**, 55 (1954).
- 15. Westerterp, K. R. and Landsman, P.: *Chem. Eng. Sci.*, **17**, 363 (1962).
- 16. Zhang, S. H., Ni, X. D. and Su, Y. F.: *Can. J. Chem. Eng.*, **59**, 573 (1981).